Electronic Supplementary Material (ESI) for Physical Chemistry Chemical Physics.

Supporting Information

Thermal Transport Properties of Graphene Aerogel as an Advanced Carrier for Enhanced Energy Storage

Jieren Song*[a], Xianghua Xu[b], Xingang Liang[b]

*E-mail: songjr_2008@126.com

[a] School of Mechanical and Material Engineering, North China University of Technology, Beijing 100144, China

[b] Key Laboratory for Thermal Science and Power Engineering of Ministry of Education, Department of Engineering Mechanics, Tsinghua University, Beijing 100084, China

S1. Non-bonded force field parameters

Table S1. Non-bonded force field parameters

Atom	ε (meV)	σ (Å)	Molecular type	Force field type
C	4.56	3.851	Graphene	Universal force field
S	17.68	3.390	Sulfur	OPLS
C	2.35	4.010	Octadecane	PCFF
H	0.87	2.995	Octadecane	PCFF

Non-bonded force field parameters are shown in Table S1. Among the non-bonded atomic interactions, the interaction of carbon in graphene with atoms in other molecules, as well as sulfur atomic interactions, are employed with a 12-6 LJ potential, while atomic interactions in octadecane molecules are adopted with a 9-6 LJ potential.

S2. Calculation of thermal conductivity of dense amorphous sulfur and octadecane

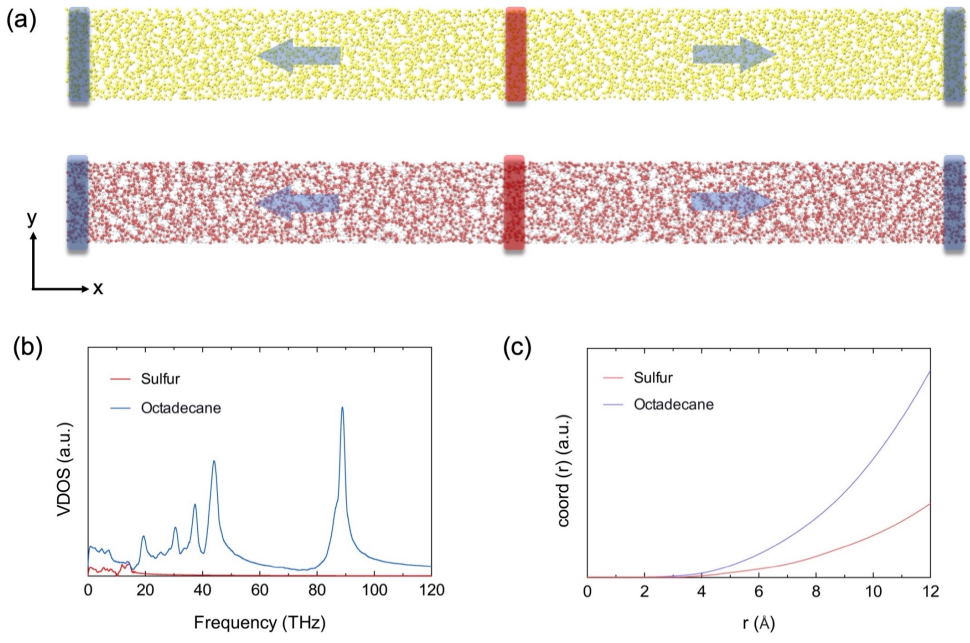

Figure S2 (a) Calculated models of thermal conductivity for dense amorphous sulfur and octadecane. (b) VDOS and (c) coordination number of dense amorphous sulfur and octadecane.

The Müller-Plathe method is used to predict the thermal conductivity of a dense amorphous sulfur and octadecane model with a length of 13 nm at room temperature, and the calculated models are displayed in Figure S2a. The parameters used to compute the thermal conductivity of the dense amorphous filler are consistent with those used for the graphene aerogel-based composite. To enhance computational efficiency and accuracy, the model height and width are set to 1/5 of the graphene aerogel model's height and width, respectively. It is confirmed that the cross-sectional area of the dense model has a negligible effect on thermal conductivity. The calculations suggest that the thermal conductivities of dense amorphous sulfur and octadecane are 0.064 and 0.103 $Wm^{-1}K^{-1}$, respectively, indicating that the thermal conductivity of dense amorphous sulfur is lower than that of octadecane. To investigate the differences in thermal transport between dense amorphous sulfur and octadecane, Figure S2b illustrates their VDOS. It can be observed that the VDOS of sulfur is significantly lower than that of octadecane, implying that amorphous sulfur has a stronger scattering of phonon defects. This is closely linked to the intrinsic structural looseness of the sulfur and octadecane models. Figure S2c demonstrates the coordination numbers of dense amorphous sulfur and octadecane, and it is found that sulfur has a lower coordination number than octadecane, indicating weaker interatomic interactions and a looser structure with fewer ligands around sulfur atoms. This looser structure in the sulfur model induces more phonon defect scattering, reducing the mean free paths of phonons, resulting in lower phonon energy transfer and, consequently, a smaller thermal conductivity in dense amorphous sulfur.

S3. Calculation of Effective Thermal Conductivity using the Maxwell-Eucken Model

The Maxwell-Eucken equation is as follows:

$$k_{eff} = k_{GA}\frac{2k_{GA} + k_f + 2V_f(k_f - k_{GA})}{2k_{GA} + k_f - V_f(k_f - k_{GA})}$$

where k_{GA} is the thermal conductivity of the matrix (GA) with embedded fillers, k_f is the thermal conductivity of the filler, and V_f is the volume fraction of the filler. The thermal conductivities for sulfur and octadecane are extrapolated, resulting in values of 0.21 and 0.35 $Wm^{-1}K^{-1}$, respectively.